Research Article

Hajer Satih Abbas*, Maadh Imad Salman Al-Rubaye, Sarra'a Dhiya'a Jaafer, Bassam farman bassam, and Abdelmajeed Alkasassbeh

Three-dimensional numerical study of the reactive powder concrete segments in tunnel lining

https://doi.org/10.1515/cls-2022-0022
Received Nov 18, 2021; accepted Feb 21, 2022

Abstract: The tunnel lining systems act as lines of defence against the forces and geotechnical situations. The use of precast concrete tunnel linings (PCTLs) has been escalating due to its effective and economical installation process. The tunnels usually suffer from the premature deterioration due to corrosion of the reinforcement and thus need maintenance. Corrosion leads to the distress in PCTL leading to the cracking and finally the scaling of concrete. This study aims to assess the structural durability performance of reactive powder concrete (RPC) as the material of tunnel lining segments compared to reinforced concrete (RC) and high performance concrete (HPC). The numerical findings indicated that the maximum load capacity of PRC-PCTL segments was greater than that of the corresponding RC and HPC segments. Regarding the findings, PRC is a very significant option for conventional segments. The high strength of PRC can decrease the thickness of the PCTL segments, resulting in the decreased material cost. Also, PRC-PCTL segments can eliminate the laborious and costly production of RC segments and mitigate the corrosion damage and thus enhance the service life of lining segments.

Keywords: reactive powder voncrete; corrosion, high compressive strength; finite-element model; tunnel segment.

1 Introduction

The use of precast concrete tunnel segments in the projects has creased due to its effective and economical utilization compared to the conventional in-situ lining appraoch [1–3]. In general, precast concrete tunnel lining (PCTL) segments are planned for more than 100 years of service life [4] with reinforced concrete (RC). Hence, several cases suffered from the premature deterioration prior to gaining their service life. It was basically assigned to the corrosion caused by chloride infiltration [5–7].

The Reactive Powder Concrete (RPC) is the ultra-high strength and ductile concrete prepared by replacing the standard aggregate with quartz powder, silica fume and steel fibers [8]. The concrete does not comprise coarse aggregates, but involves cement, silica foam, sand, powdered quartz, superplasticizer, and steel fiber. Avoiding the inclusion of coarse aggregates by the inventors is a significant aspect of the microstructure and function of RPC which decreases the heterogeneity in mortar and aggregate mix. The additives, lack of coarse aggregates, small water-to-cement ratio, fine steel fibers, heat treatment, and compression before and after setting are the RPC's fundamental features [9–14]. The compressive RPC strength is in the 200–800 MPa range, its flexural strength is from 30 to 50 MPa, and its Young's modulus around 50–60 GPa [15–19]. Because of RPC's durability and excellent mechani properties, its utilizations are expanded. RPC structural elements are resistant against chemical attack, impact loads (with collision with vehicles and vessels), and sudden kinetic loads based on the earthquakes. Made up of compact and ordered hydrates, RPC is basically characterized by high performance. The microstructure is optimized by accurate particle gradation to maximize density. RPC heavily relies on the pozzolanic features of the washed silica foam and the optimizing cement concrete to gain the maximum hydrate [20–27]. Thus, PRC can be proven to be a more long-lasting material for precast concrete tunnel lining construction. Besides to enhancing the mechanical and durability features, the replacement of reinforcement with PRC in tunnel segments can delete the laborious and costly construction of tunnel segments. Moreover, PRC lining segments' cross-sectional dimensions can be decreased due to their high strength, leading to economical fabrication. Multiple research investigated the flexural capacity of conventional

***Corresponding Author: Hajer Satih Abbas:** Civil Engineering department, Al-Esraa university college, Baghdad, Iraq; Email: dr.hajer@esraa.edu.iq
Maadh Imad Salman Al-Rubaye, Sarra'a Dhiya'a Jaafer, Bassam farman bassam: Civil Engineering department, Al-Esraa university college, Baghdad, Iraq
Abdelmajeed Alkasassbeh: Civil engineering department, Faculty of Engineering, Al al-Bayt University, Mafraq 25113, Jordan

RC tunnel segments [28–33]. The corrosion deterioration of conventional RC-PCTL has resulted in developing the reactive powder concrete (PRC) tunnel lining segments. Hence, the present research obtains an evaluation of the mechanical behaviour of reactive powder concrete (RPC) tunnel lining segments. This study aims to assess the structural and durability function of reactive powder concrete (RPC) tunnel lining segments compared to reinforced concrete (RC) and high performance concrete (HPC). Furthermore, finite element analysis using ABAQUS was conducted in order to verify the experimental behaviour and comparison of the performance of RPC with RC and HPC tunnel lining segments was presented in this study.

2 RPC in comparison with HPC

A comparison between mechanical and durability properties of the RPC and (high performance concrete) HPC shows the RPC to offer a higher compressive strength and a permeability lower than the HPC. The HPC is a product of novel concrete science, which uses additives and scientific techniques to control the concrete's microstructure [34, 35].

Owing to its microstructure, the HPC has achieved its maximum compressive strength. Nonetheless, at any given strength, coarse aggregates are the weakest links in the concrete structure. The only remaining solution to further increase the compression strength of the concrete is to remove coarse aggregates, which is the same approach that has been adopted in developing the RPC. Table 1 compares the mechanical properties of the typical RPC with a regular HPC with an 80 MPa compressive strength. The higher fracture toughn of the RPC is suggestive of its better ductility. Aside from the mechanical properties, RPCs have an exceptionally dense microstructure that makes them impermeable to water and durable.

Thanks to its low porosity and permeability, restricted contraction, and high corrosion resistance, the RPC offers remarkable durability. Compared to the HPC, the RPC passes no liquid or gas through. The RPC specifications listed under Table 2 enable it to be used in aggressive chemical environments and applications where other types of concrete do not last long due to wear and tear. Results indicate that RC and HPC concretes are more vulnerable to corrosion problem compared with RPC concrete.

Table 1: Mechanical properties of RPC vs. HPC

SPECIFICATIONS	HPC	RPC
Compression capacity (MPa)	85~100	200~800
Flexural capacity (MPa)	6~8	45-60
Modulus of elasticity (GPa)	35~40	70
Fracture toughness (J/m^2)	<1000	30000

Table 2: The durability of RPC vs. HPC

Characteristic	Value
Wear	2~2.5 times less
Absorption of water	6.5~7.5 times less
Rate of corrosion	7~8.5 times less
Diffusion of chloride ions	20~30 times less

3 Numerical verification

The finite-element software, ABAQUS [36] was applied for model verification, contrasting the findings with the experimental surveys of Abbas [37].

3.1 Model geometry

Figure 1 illustrates the model geometry, and the meshed model is presented in Figure 2. The model was meshed using square elements with a length-to-width ratio of 1, as it has been suggested that they produce the best results

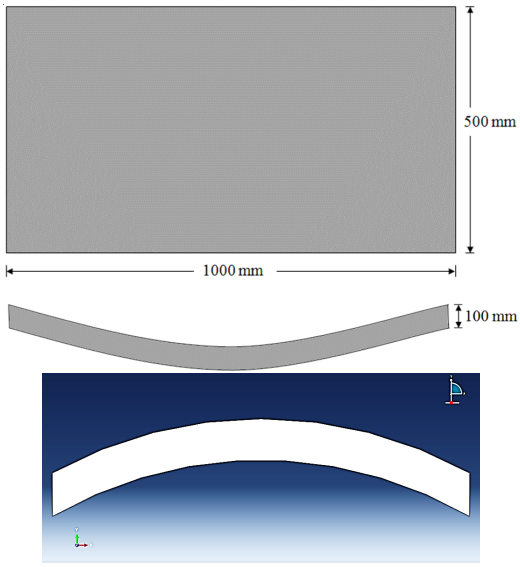

Figure 1: 2D model geometry

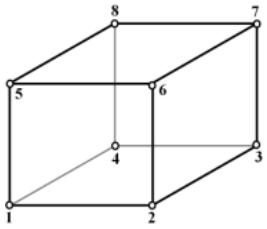

8-node brick element

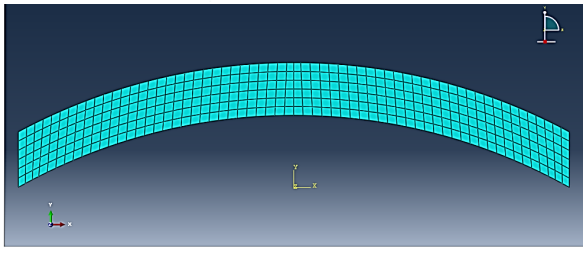

Figure 2: Meshed 2D model

in the finite-element method. The eight-node linear brick element C3D8R was used for modeling (Figure 2).

3.2 Model boundary conditions

As depicted in Figure 3, support conditions were defined for the model by fixing the model in the vertical direction (Figure 4) at the points where the segment is in contact with two bottom frames (reaction). Further, a vertical downward velocity was defined for the upper part of the segment (Figure 5) for flexural loading.

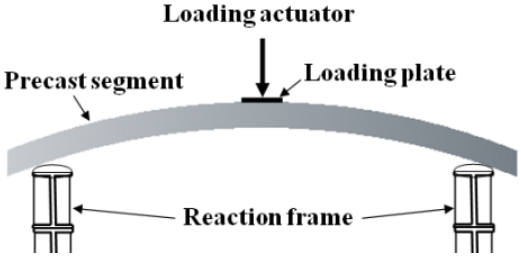

Figure 3: Experimental boundary conditions in the lower part of the segment Abbas [37]

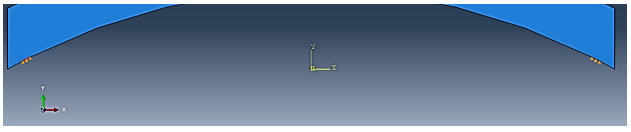

Figure 4: Numerical boundary conditions in the lower part of the segment

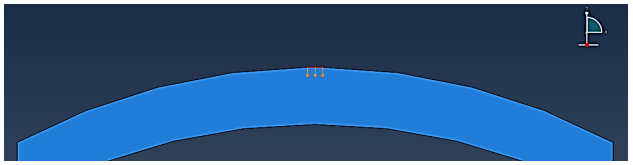

Figure 5: Numerical boundary conditions in the upper part of the segment

A critical parameter in the finite-element techniques is the solution time and complexity, which depend on the shape and number of elements. In light of the above discussions, different types of mesh were used in modeling the studied tunnel segment. It was found that similarly acceptable results are obtained by using 50 and 25 mm elements. Therefore, the 50 mm elements were used for the shorter analysis time (Figure 6).

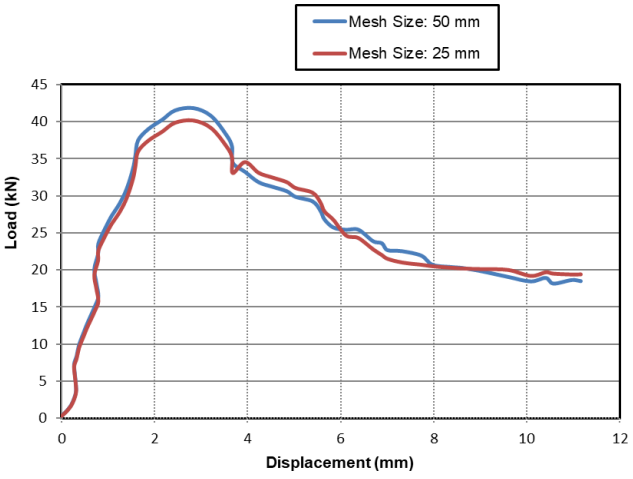

Figure 6: Load-displacement curve of the model with two mesh sizes

3.3 Result validation

The current numerical ABAQUS [36] model (Figure 6) was contrasted with the load-displacement curve of the flexural test in the work of Abbas [37] (Figure 7) at the point of loading for validation. The two curves are plotted on the same graph in Figure 8 for a better comparison. Comparing two curves indicate the consistency of this study's findings with those of Abbas [37].

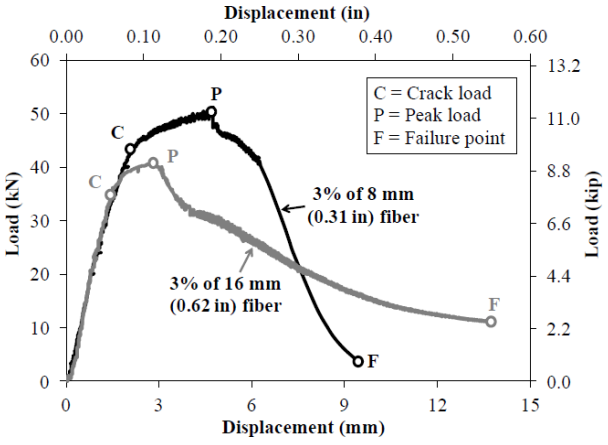

Figure 7: Load-displacement curve from flexural testing Abbas [37]

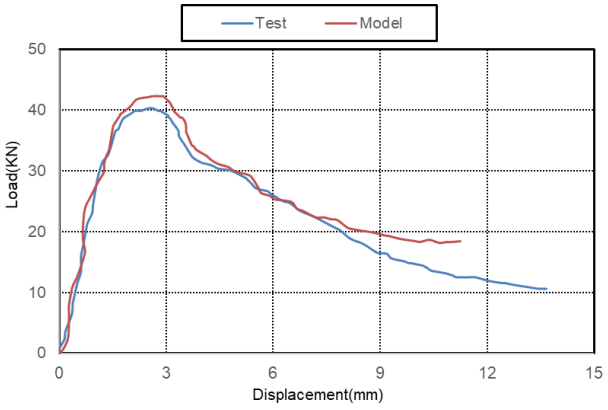

Figure 8: A comparison of the load-displacement curves

Table 3: The details of developed models

Model no.	Lining type	Tunnel overhead-side (kPa)	Tunnel overhead-top (kPa)
T0	RPC	25	20
T1	UHPC	25	20
T2	HPC	25	20
T3	RC	25	20

4 Optimizing the tunnel segments with RPC

In this section, the impact of incorporating the RPC in the tunnel segments are studied with 3D modeling. To this objective, a 3D model of subway tunnel with actual dimension was developed applying ABAQUS [36] Figure 9 indicates the segment model with the details about the overhead, tunnel diameter, and lining thickness. Table 3 shows the details of developed models.

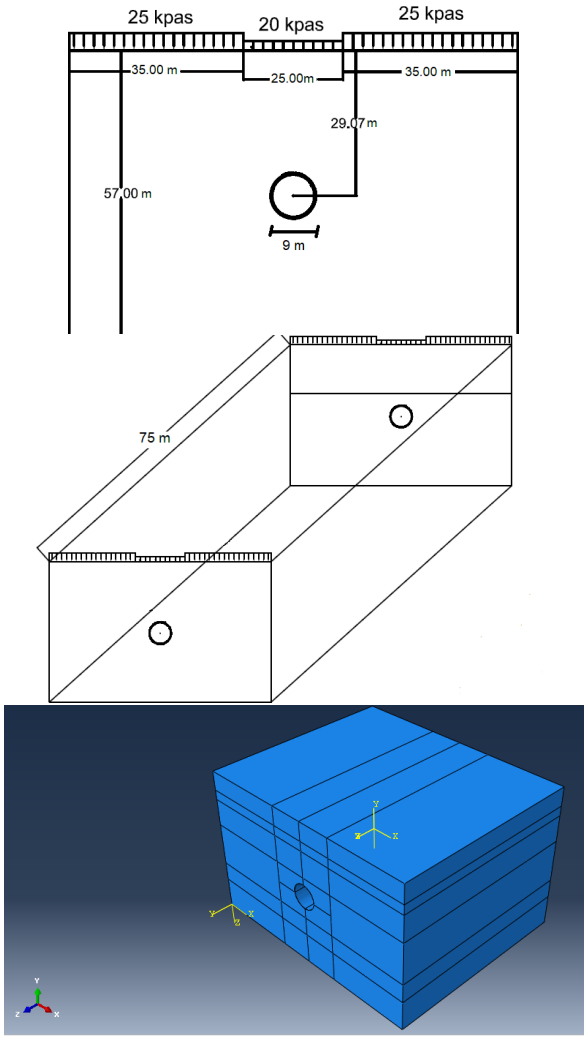

Figure 9: Model geometry

4.1 Model geometry and meshing

Figure 9 illustrates the model geometry, and the meshed model is presented in Figure 10. The model comprises six layers of three different materials. The model was meshed considering the two following points: First, square elements (with a length-to-width ratio of 1) were used for meshing, as they have been recommended for producing the best results in the finite-element method. Second, a finer mesh was used for the tunnel due to the considerable displacement and stress concentration (Figure 11). On the other hand, a smaller element with finer mesh will be closer to representing distributed loading type, as the nodes will be closer to the locations of the contact. In addition, as a general principle of any numerical method, the finer the discretization the closer it is to the exact solution.

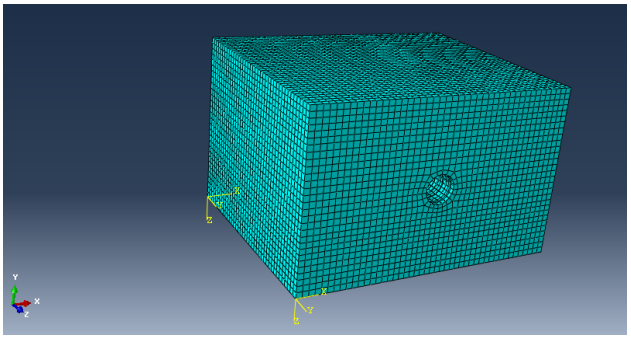

Figure 10: Model meshing

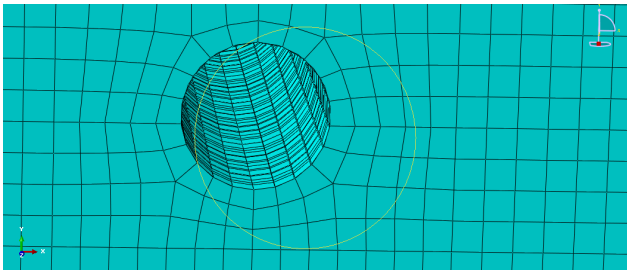

Figure 11: Finer mesh around the tunnel

4.2 Material and element specifications

Table 4 lists the specifications of the materials used to model soil layers. As evident, elastic modulus, Poisson's ratio, cohesion, and internal friction angle are necessary to model the soil. The linearly elastic-perfectly plastic model using the Coulomb constitutive law was used to represent the soil.

Further, the concrete was modeled using the linear elastic relationship based on Table 5. In this case, the elastic modulus, Poisson's ratio, and the specimens' compressive strength are necessary. Interactions between the soil and the concrete cover were modeled as follows:

Tangential behavior: The tangential behavior between the soil and the concrete followed Coulomb's friction law in zero-cohesion conditions with a $\mu = 100$ ($\phi = 89.43°$) coefficient of friction (Figure 12a). This relationship has been recommended by the ABAQUS [36].

Vertical Behavior: The hard contact relation was used to model the vertical behavior, as evident from the figure below. This configuration allows for the vertical transfer of stress in case of contact between two surfaces. The model does not account for tensile stress (Figure 12b).

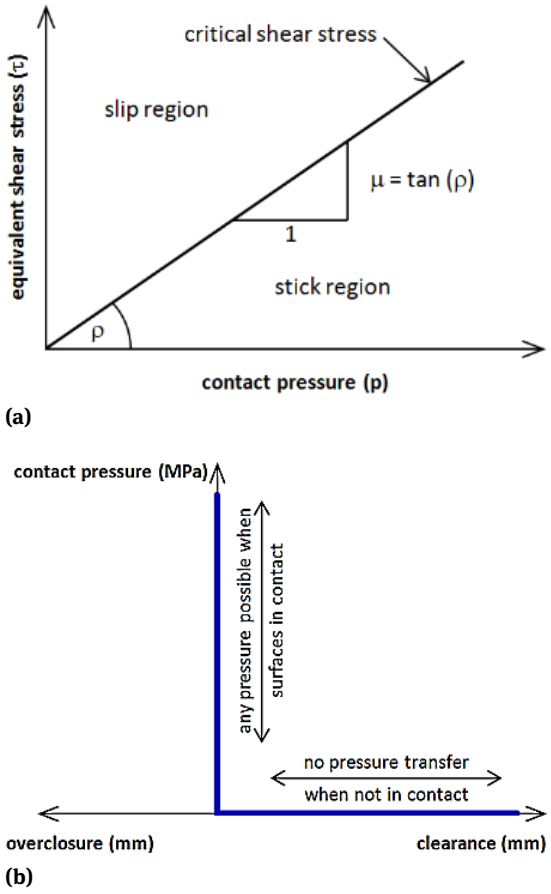

Figure 12: Coulomb friction law and vertical behavior between the soil and the concrete (hard contact) ABAQUS (2012)

4.3 Model boundary conditions

The support conditions were defined to fix the displacement and rotation of the model's bottom in the horizontal and vertical directions. Further, the sides were fixed in the horizontal direction. Figure 13 shows the defined boundary conditions. The boundaries have been placed far enough from the tunnel to ensure that the boundaries have negligible effects in modeling.

4.4 Initial conditions of the model

The initial conditions of the problem include in-situ stresses and groundwater conditions. According to Figure 14, the model assumes a 19.65 m water table. The model's pore water pressure was based on the water level. In the first stage, static analysis, in-situ stresses were created in the model.

Table 4: Soil layer specifications

	Permeability (m/s)	Dry density (kN/m^3)	Poisson's ratio	Elastic modulus (MPa)	Internal friction angle (°)	Cohesion (kPa)
ET1 Layer	9e−7	18.4	0.3	75	31	18
ET2 Layer	9e−7	19	0.32	50	28	35
ET3 Layer	9e−7	17	0.35	35	24	31

Table 5: Concrete specifications in the models

Model no.	Lining type	Elastic modulus (GPa)	Compressive strength (MPa)	Poisson's ratio
T0	RPC	55	200	0.1
T1	UHPC	37	100	0.15
T2	HPC	35	80	0.15
T3	RC	20	25	0.2

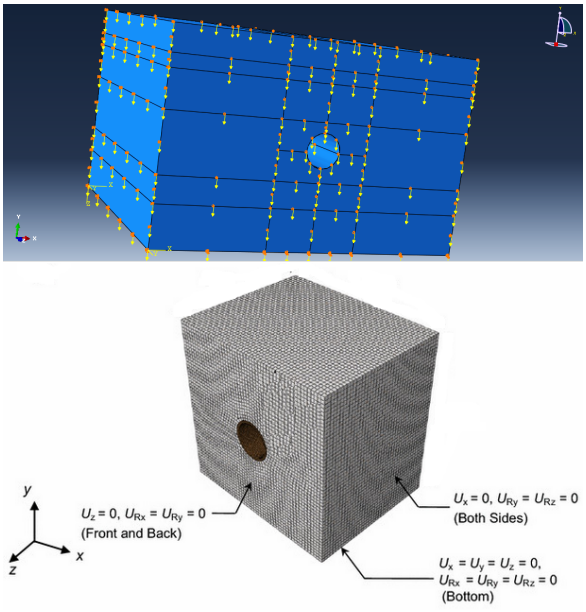

Figure 13: Boundary conditions on the sides

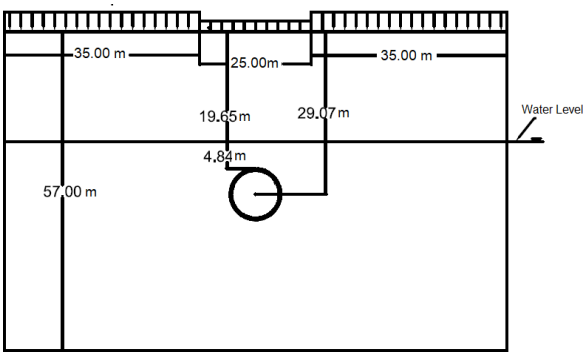

Figure 14: Groundwater conditions in the model

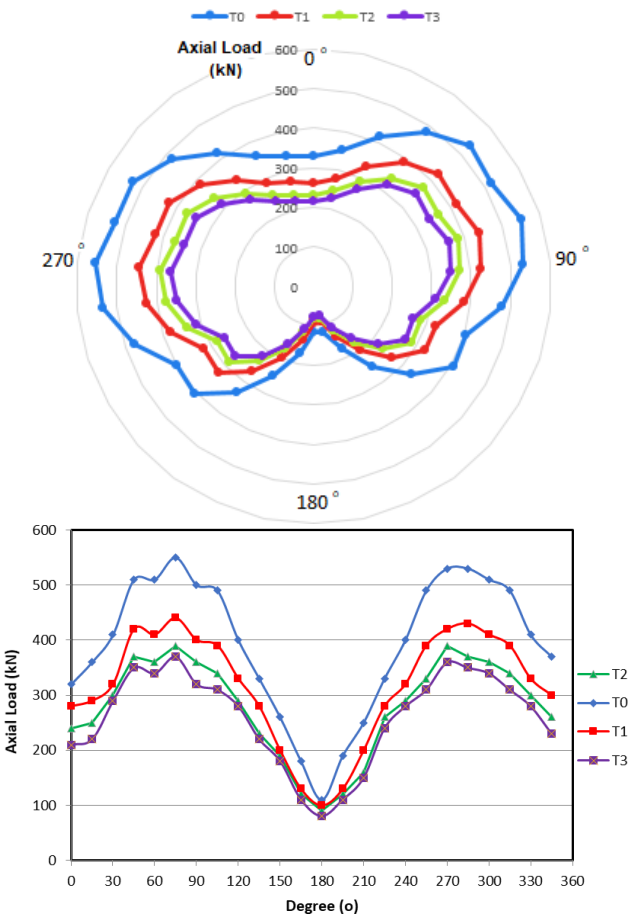

Figure 15: Comparing the axial force in different models

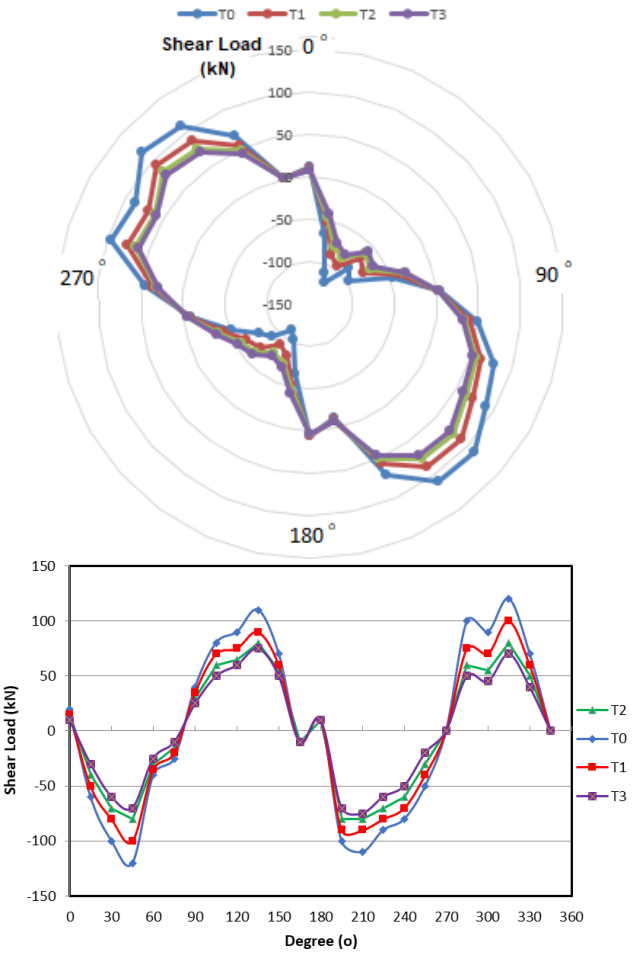

Figure 16: Comparing the shear force in different models

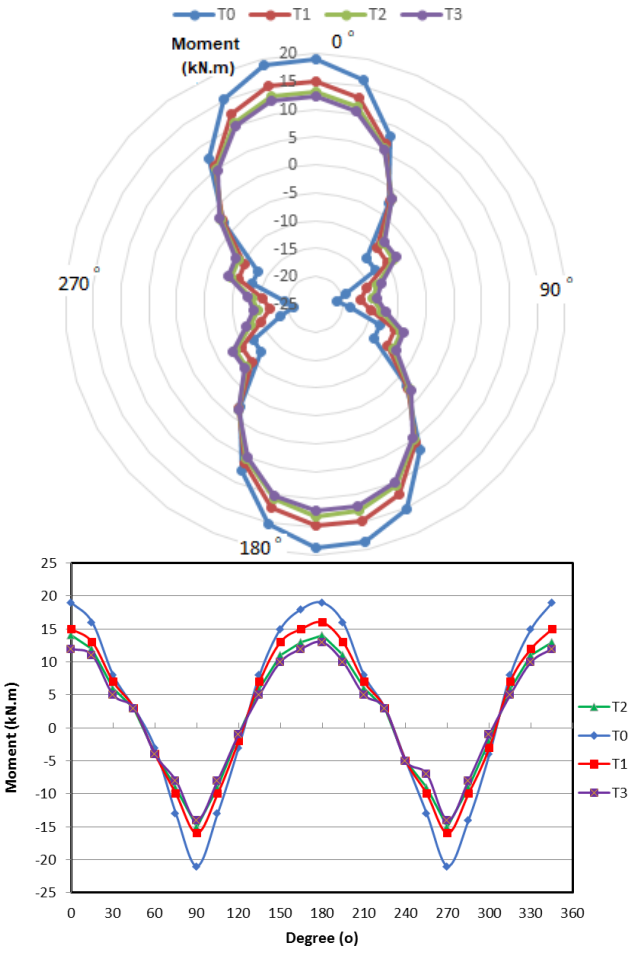

Figure 17: Comparing the bending moment in different models

4.5 Results analysis

4.5.1 Axial force on the tunnel lining

The axial force on the tunnel lining for multiple segments is plotted in Figure 15. The values in the figure are in kN. Based on Figure 15, substituting the RC with the RPC enhances the maximum axial force which the tunnel lining can withstand. The findings indicate that the maximum axial force corresponds to RPC and the minimum axial force to the RC concrete. Hence, RPC withstands 48, 38, and 20% higher axial force than RC, HPC, and UHPC, respectively. Thus, considering the RPC's excellent performance, a smaller segment thickness can be regarded in the design than with other kinds of concrete.

4.5.2 Shear force on the tunnel lining

The shear force on the tunnel lining for multiple segments is plotted in Figure 16. The amounts in the figure are in kN. The maximum shear in the models corresponds to the case with the RPC and is about 30% higher than other kinds of concrete. Almost the same shear force is exerted on the tunnel lining in the other cases, and similarly to the argument made about the axial force, the higher shear capacity aids make lighter tunnel segments.

4.5.3 Bending moment on the tunnel lining

The bending moment on the tunnel lining for different segments is plotted in Figure 17. The values in the figure are in kN·m. The findings indicate that the maximum axial force corresponds to the RPC and the minimum axial force to the regular concrete. A same argument to that created for the shear stress on the tunnel lining holds for the bending moment, as the higher control over the displacements and the deformation around the tunnel increases the maximum bending moment in the case of the reinforced concrete. Moreover, RPC withstands 46, 48, and 26% higher axial

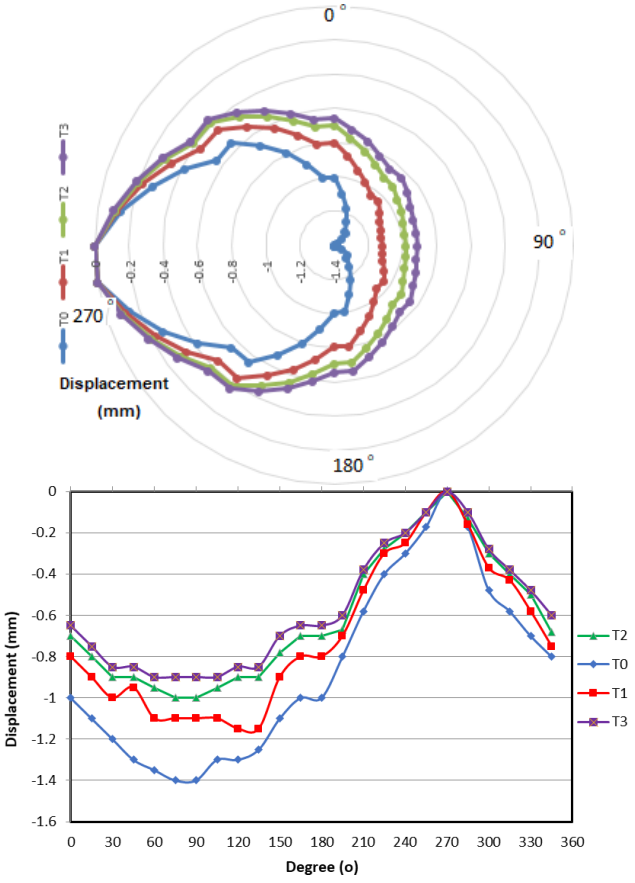

Figure 18: Horizontal displacement on the tunnel lining in different models

force than regular concrete, HPC, and UHPC, respectively. Thus, given the RPC's excellent performance, a smaller segment thickness can be regarded in the design than with other kinds of concrete.

4.5.4 Displacement on the tunnel lining

The displacement on the tunnel lining in multiple cases is plotted in Figure 18. Considering the displacement symmetry on the tunnel lining, the figure plots the displacement for only half of the tunnel segment. The values in the figures are in mm. It is clear from Figure 18 that horizontal displacement of tunnel lining is decreased by reinforcing the tunnel segment with RPC.

5 Conclusions

The impacts of applying the RPC in a tunnel segment were surveyed by 3D modeling utilizing the finite-element software ABAQUS. The numerical models were approved via experimental results. Results show that reinforced concrete-PCTL segments are more vulnerable to corrosion problem compared with RPC-PCTL. The numerical findings indicated that the compressive strength of PRC segments was greater than that of the RC and HPC segments. Regarding the findings, PRC is a very significant option for conventional RC-PCTL segments. Very high strength of PRC can permit decreasing the thickness of PCTL segments, resulting in the decreased material cost and more sustainable fabrication. Besides, PRC-PCTL segments can delete the laborious and costly manufacturing of RC segments which mitigates the corrosion damage, resulting in the improved service life of tunnel segments. The findings indicate that the maximum axial force corresponds to the RPC and the minimum axial force to the conventional RC. The same argument to which created for the shear stress on the tunnel lining holds for the bending moment, as the higher control over the displacements and the deformation around the tunnel increases the maximum bending moment in the case of the reinforced concrete. Moreover, the RPC withstands 48, 38, and 20% higher axial force than RC, HPC, and UHPC, respectively. Hence, considering the RPC's excellent performance, a smaller segment thickness can be regarded in the design than with other kinds of concrete.

Funding information: The authors state no funding involved.

Author contributions: All authors have accepted responsibility for the entire content of this manuscript and approved its submission.

Conflict of interest: The authors state no conflict of interest.

References

[1] Elliott K. Precast Concrete Structures. 1st Ed. Boston, USA: Butterworth-Heinemann; 2002.
[2] Wang S, Jiang X, Bai Y. The influence of hand hole on the ultimate strength and crack pattern of shield tunnel segment joints by scaled model test. Front Struct Civ Eng. 2019 Oct;13(5):1200–13.
[3] Ma B, Zou D, Xu L. Manufacturing technique and performance of functionally graded concrete segment in shield tunnel. Front Archit Civ Eng China. 2009 Mar;3(1):101–4.
[4] Hung JC, National Highway Institute (US), Parsons, Brinckerhoff, Quade & Douglas. Technical manual for design and construction of road tunnels—civil elements. AASHTO; 2010.
[5] ITA Working Group on Maintenance and Repair of Underground Structures. Report on the damaging effects of water on tunnels

during their working life. Tunn Undergr Space Technol. 1991 Jan;6(1):11–76.
[6] Usman M, Galler R. Long-term deterioration of lining in tunnels. Int J Rock Mech Min Sci. 2013 Dec;64:84–9.
[7] Zhiqiang Z, Mansoor YA. Evaluating the strength of corroded tunnel lining under limiting corrosion conditions. Tunn Undergr Space Technol. 2013 Sep;38:464–75.
[8] Richard P, Cheyrezy M. Composition of reactive powder concretes. Cement Concr Res. 1995 Oct;25(7):1501–11.
[9] Aydin S, Baradan B. Engineering properties of reactive powder concrete without Portland cement. ACI Mater J. 2013 Nov;110(6):619.
[10] Kushartomo W, Bali I, Sulaiman B. Mechanical behavior of reactive powder concrete with glass powder substitute. Procedia Eng. 2015 Jan;125:617–22.
[11] Maroliya MK. Mechanical behavior of modified of reactive powder concrete. Int J Eng Res Appl. 2012 Sep;2(5):2062–7.
[12] Cwirzen A, Penttala V, Vornanen C. Reactive powder based concretes: mechanical properties, durability and hybrid use with OPC. Cement Concr Res. 2008 Oct;38(10):1217–26.
[13] Cwirzen A. The effect of the heat-treatment regime on the properties of reactive powder concrete. Adv Cement Res. 2007 Jan;19(1):25–33.
[14] Kadhem E, Ali A, Tobeia S. Experimental comparative study of reactive powder concrete: Mechanical properties and the effective factors. The 3^{rd} International Conference on Buildings, Construction and Environmental Engineering; 2017 Oct 23-25; Sharm el-Shiekh. EDP Sciences; 2018;162:04004.
[15] Nematzadeh M, Poorhosein R. Estimating properties of reactive powder concrete containing hybrid fibers using UPV. Comput. Concrete. 2017 Oct 1;20(4):491-502.
[16] Ji T, Yang Y, Fu MY, Chen BC, Wu HC. Optimum Design of Reactive Powder Concrete Mixture Proportion Based on Artificial Neural and Harmony Search Algorithm. ACI Mater J. 2017 Jan;114(1).
[17] Sun H, Li Z, Memon SA, Zhang Q, Wang Y, Liu B, et al. Influence of ultrafine $2CaO{\cdot}SiO_2$ powder on hydration properties of reactive powder concrete. Materials (Basel). 2015 Sep;8(9):6195–207.
[18] Yang J, Jinhui L, Hongbin L, Kaipei T, Zhishun G. On the thermal spalling mechanism of reactive powder concrete exposed to high temperature: numerical and experimental studies. Int J Heat Mass Transf. 2016;98;493–507.
[19] Ghaffari Moghaddam F, Akbarpour A, Firouzi A. Dynamic modulus of elasticity and compressive strength evaluations of modified reactive powder concrete (MRPC) by non-destructive ultrasonic pulse velocity method. J Asian Archit Build Eng. 2021 Feb;21(2):490–499.
[20] Grzeszczyk S, Matuszek-Chmurowska A, Černý R, Vejmelková E. Mikrostruktura betonów z proszków reaktywnych. Cem Wapno Beton. 2018;21/83(1):1–15.
[21] Salman BF, Al-Rumaithi A, Al-Sherrawi MH. Properties of Reactive Powder Concrete with Different Types of Cement. IJCIET. 2018 Oct;9(10):1313–21.
[22] Poorhosein R, Nematzadeh M. Mechanical behavior of hybrid steel-PVA fibers reinforced reactive powder concrete. Comput Concr. 2018;21(2):167–79.
[23] Wang D, Shi C, Farzadnia N, Shi Z, Jia H. A review on effects of limestone powder on the properties of concrete. Constr Build Mater. 2018 Dec;192:153–66.
[24] Abid M, Hou X, Zheng W, Hussain RR. High temperature and residual properties of reactive powder concrete–A review. Constr Build Mater. 2017 Aug;147:339–51.
[25] Zong-cai D, Daud JR, Chang-xing Y. Bonding between high strength rebar and reactive powder concrete. Comput Concr. 2014 Mar;13(3):411–21.
[26] Lai J, Sun W. Dynamic tensile behaviour of reactive powder concrete by Hopkinson bar experiments and numerical simulation. Comput Concr. 2010;7(1):83–6.
[27] Hwang CL, Hsieh SL. The effect of fly ash/slag on the property of reactive powder mortar designed by using Fuller's ideal curve and error function. Comput Concr. 2007;4(6):425–36.
[28] Nakamura M, Hirosawa N, Yamaguchi T, Nishida K. New Mechanical Joint Segment Tunnel Lining System. Nippon Steel Technical Report. 1998;(77-78):40–6.
[29] Mashimo H, Isago N, Yoshinaga S, Shiroma H, Baba K. Experimental investigation on load-carrying capacity of concrete tunnel lining. 28^{th} ITA General Assembly and World Tunnel Congress; 2002 Mar 2-8 Sydney, Australia. Institution of Engineers; 2002. p. 808–817.
[30] Nishikawa K. Development of a prestressed and precast concrete segmental lining. Tunn Undergr Space Technol. 2003 Apr;18(2-3):243–51.
[31] Yan G, Zhu H. Experimental study on mechanical behaviour of tunnel lining under after fire scenario. In Barták J, Hrdina I, Romancov G, Zlámal J, editors. Proceedings of the 33th ITA-AITES General Assembly and World Tunnel Congress: Underground Space – the 4th Dimension of Metropolises; 2007 May 5-10; Prague, Czech Republic. London/ Leiden/ New York/ Philadelphia/ Singapore: Taylor & Francis; 2007;1:1805-1809.
[32] Poh J, Tan KH, Peterson GL, Wen D. Structural testing of steel fibre reinforced concrete (SFRC) tunnel lining segments in Singapore. Singapore: Land Transport Authority; 2009.
[33] Caratelli A, Meda A, Rinaldi Z, Romualdi P. Structural behaviour of precast tunnel segments in fiber reinforced concrete. Tunn Undergr Space Technol. 2011 Mar;26(2):284–91.
[34] Qi J, Hu Y, Wang J, Li W. Behavior and strength of headed stud shear connectors in ultra-high performance concrete of composite bridges. Front Struct Civ Eng. 2019 Oct;13(5):1138–49.
[35] Landis EN, Kravchuk R, Loshkov D. Experimental investigations of internal energy dissipation during fracture of fiber-reinforced ultra-high-performance concrete. Front Struct Civ Eng. 2019 Feb;13(1):190–200.
[36] Zhang J, Li J. Investigation into Lubliner yield criterion of concrete for 3D simulation. Eng Struct. 2012 Nov;44:122–7.
[37] Abbas S. Structural and durability performance of precast segmental tunnel linings [dissertation]. London (ON): The University of Western Ontario; 2014.